

RESEARCH ARTICLE

10.1002/2017JD027070

Key Points:

- Snow albedo reductions induced by black carbon (BC) and other light-absorbing particles (LAPs) are quantified based on large-area field surveys
- Non-BC LAPs are abundant enough to affect the estimation of BC-in-snow albedo reduction and should be included in climate model simulations
- Albedo reductions calculated using a two-layer snow radiative transfer model agree reasonably with that calculated using a multilayer model

Correspondence to:

C. Dang,
chengd1@uw.edu

Citation:

Dang, C., S. G. Warren, Q. Fu, S. J. Doherty, M. Sturm, and J. Su (2017), Measurements of light-absorbing particles in snow across the Arctic, North America, and China: Effects on surface albedo, *J. Geophys. Res. Atmos.*, 122, doi:10.1002/2017JD027070.

Received 3 MAY 2017

Accepted 3 AUG 2017

Accepted article online 5 AUG 2017

Measurements of light-absorbing particles in snow across the Arctic, North America, and China: Effects on surface albedo

Cheng Dang¹ , Stephen G. Warren¹, Qiang Fu¹ , Sarah J. Doherty^{1,2} , Matthew Sturm³ , and Jing Su⁴

¹Department of Atmospheric Sciences, University of Washington, Seattle, Washington, USA, ²Joint Institute for the Study of Atmosphere and Ocean, University of Washington, Seattle, Washington, USA, ³Geophysical Institute, University of Alaska Fairbanks, Fairbanks, Alaska, USA, ⁴Key Laboratory for Semi-Arid Climate Change of the Ministry of Education and College of Atmospheric Sciences, Lanzhou University, Lanzhou, P.R. China

Abstract Using field observations, we perform radiative transfer calculations on snowpacks in the Arctic, China, and North America to quantify the impact of light-absorbing particles (LAPs) on snow albedo and its sensitivity to different factors. For new snow, the regional-averaged albedo reductions caused by all LAPs in the Arctic, North America, and China are 0.009, 0.012, and 0.077, respectively, of which the albedo reductions caused by black carbon (BC) alone are 0.005, 0.005, and 0.031, corresponding to a positive radiative forcing of 0.06, 0.3, and 3 W m⁻². For the same particulate concentrations, the albedo reduction for old melting snow is larger than that of new snow by a factor of 2; this leads to 3–8 times larger radiative forcing, in part due to higher solar irradiance in the melting season. These calculations used ambient snowpack properties; if all snowpacks were instead assumed to be optically thick, the albedo reduction would be 20–50% larger for new snow in the Arctic and North America and 120–300% larger for old snow. Accounting for non-BC LAPs reduces the albedo reduction by BC in the Arctic, North America, and China by 32%, 29%, and 70%, respectively, for new snow and 11%, 7%, and 51% for old snow. BC-in-snow albedo reduction computed using a two-layer model agrees reasonably with that computed using a multilayer model. Biases in BC concentration or snow depth often lead to nonlinear biases in BC-induced albedo reduction.

Plain Language Summary The presence of certain particles in snow darkens the snowpack by increasing sunlight absorption, which leads to earlier snowmelt. This darkening can also affect regional climate. In this work, we use field observational data gathered from the Northern Hemisphere (the Arctic, China, and North America) and a physical model to quantify the impact of these particles on snow reflectivity, and we examine the dependence of these impacts on different factors such as snow depth and particle concentration.

1. Introduction

Over the past decade, our group and collaborators have carried out multiple large-area snow surveys in the midlatitudes and high latitudes of the Northern Hemisphere, specifically in the Arctic [Doherty *et al.*, 2010], Northern China [Huang *et al.*, 2011; Wang *et al.*, 2013], and North America [Doherty *et al.*, 2014; Dang and Hegg, 2014; Doherty *et al.*, 2016]. The objective was to quantify the concentrations of light-absorbing particles (LAPs) in snow across these regions.

LAPs, by definition, absorb solar radiation. In contrast to light-scattering particles like sulfate aerosols, which cool the atmosphere and surface by reflecting incoming solar radiation or increasing cloud reflectivity [Charlson *et al.*, 1992], LAPs in the atmosphere absorb solar radiation and heat the absorbing aerosol layer. Depending on the vertical profile of LAPs, the imposed heating may evaporate clouds, enhance or suppress vertical motions, and change the climate dynamics [Koch and Del Genio, 2010]. These LAPs can be removed from the atmosphere by dry and/or wet deposition [Bond and Bergstrom, 2006]. After LAPs are deposited on bright surfaces like snow, they reduce the albedo [Warren and Wiscombe, 1980].

One of the major LAPs in snow is black carbon (BC). BC is a unique carbonaceous aerosol that absorbs strongly across the ultraviolet (UV) and visible wavelength bands [Bond *et al.*, 2013]; a small amount of BC can reduce snow albedo significantly because ice itself is almost nonabsorbing at these wavelengths [Warren and Wiscombe, 1980]. BC results from incomplete combustion; its dominant emitters vary by

location. Globally, about 60% of BC is emitted from energy-related combustion and the rest from biomass burning [Bond *et al.*, 2013]. A large fraction of BC is emitted from anthropogenic sources, and it has a high mass-absorption coefficient. Because of this, BC is recognized as an important forcing agent in regional and global climate. The impact of BC on snow was first highlighted by Warren and Wiscombe [1980, 1985], and it was later incorporated into climate models by Hansen and Nazarenko [2004], who estimated the BC-in-snow/ice radiative forcing in the Northern Hemisphere. In a recent assessment, the globally averaged BC-in-snow effective forcing (i.e., including rapid adjustments) is estimated to be 0.1 W/m^2 [Bond *et al.*, 2013].

Besides BC, there are other types of light-absorbing particles in snow, most notably brown carbon (BrC) and mineral dust (MD) [e.g., Moosmüller *et al.*, 2009; Bond *et al.*, 2004; Kirchstetter *et al.*, 2004]. At the regional scale, especially in areas downwind of desert and semiarid regions, MD can dominate the light-absorption by LAPs, for example, in Colorado [Painter *et al.*, 2007], Inner Mongolia [Wang *et al.*, 2013], and Japan [Aoki *et al.*, 2006]. The so-called brown carbon (BrC) is the light-absorbing portion of primary organic carbon or secondary organic aerosols. Primary BrC is often coemitted with BC from combustion sources or is present in soil (humic-like substances [Dang and Hegg, 2014]), plants, and other natural noncombustion sources. Secondary BrC is formed from the atmospheric transformation of organic species [Andreae and Gelencsér, 2006]. The contribution of BrC to snow-albedo reduction is smaller but also significant [Wang *et al.*, 2015]. In this work, we will refer to BrC and MD as non-BC LAPs collectively.

Given the potentially significant impact of LAPs on snow albedo, many model simulations have been done to estimate the climate forcing induced by BC in snow and some on the impact of non-BC LAPs. These model studies either (1) prescribe fixed snow-albedo reductions across large areas in different regions [Hansen and Nazarenko, 2004] or (2) simulate the BC deposition in snow and calculate their induced albedo reductions [Jacobson, 2004; Flanner *et al.*, 2007, 2009; Qian *et al.*, 2009, 2011; Zhao *et al.*, 2014; Namazi *et al.*, 2015]. However, the complex nature of LAPs (diverse emission sources, chemical species, and transport scales) adds difficulty and uncertainty to model simulations of LAP concentrations [Moosmüller *et al.*, 2009; Bond *et al.*, 2013]. The aforementioned field campaigns are thus useful sources of observational data sets on light-absorbing particles in snow across these areas.

During the field campaigns, snow samples were collected, processed, and measured using the same techniques across all campaigns; the major outputs are snow depth, BC concentration, and fractional absorption by non-BC LAPs. Vertical profiles of LAPs were obtained at most of these sites. The data from these campaigns are publicly available in publications [Doherty *et al.*, 2010; Wang *et al.*, 2013; Doherty *et al.*, 2014] for scientific studies and can be downloaded from the websites <http://www.atmos.washington.edu/articles/BCArcticSnow/> and http://www.atmos.washington.edu/articles/BC_LAP_Snow_FieldData/. So far, the major use of these data has been for model evaluations.

In the Arctic, the modeled BC in snow by Koch *et al.* [2009] was generally lower by a factor of 0.3–1 than that observed by Doherty *et al.* [2010], while the modeled BC mixing ratio by Flanner *et al.* [2009] was lower in some locations and higher in others, being different from the observations by factors of 0.6 to 3.4. These results, as well as the results of other measurement/model comparisons in the Arctic, are summarized in Table 21 of Bond *et al.* [2013]. In China, compared with the observations of Wang *et al.* [2013], Zhao *et al.* [2014] found that Weather Research and Forecasting model coupled with Chemistry (WRF-Chem) underestimates the surface-layer BC in the clean regions but significantly overestimates it in polluted regions. In North America, Zhang *et al.* [2015] pointed out that the Community Atmosphere Model version 5 (CAM 5) has a significant low bias in the predicted mixing ratio of BC in snow. Namazi *et al.* [2015] simulated the BC-in-snow mixing ratio using the Canadian Atmospheric Global Climate Model, concluding that the model agrees with observations within an order of magnitude across the Northern Hemisphere. Almost all these validations focused on BC, some on MD, and only one on BrC.

In general, the modeled BC agrees with observations within an order of magnitude. Constrained by the temporal and spatial resolutions of model simulations, most of these comparisons suffer from mismatches in time and/or locations, complicating interpretation of these comparisons [Qian *et al.*, 2015]. Depending on the research purpose, the impact of such uncertainty on modeling results can be either major or minor. For model simulations aiming for a better evaluation of radiative forcing induced by LAPs in snow, comparison with the measured BC concentration is just the first step. For a given BC concentration the simulated BC-induced radiative forcing might also be affected by other factors and processes.

First, the direct albedo reduction caused by LAPs in snow is influenced by factors other than LAP concentration, including snow depth, snow grain size and shape, cloud cover, and cloud optical depth [Warren and Wiscombe, 1980; Aoki *et al.*, 2011; Dang *et al.*, 2015, 2016]. Incorrect simulation of these factors can yield errors in snow albedo similar to or greater than the albedo reduction caused by LAPs. Model validation should include these factors as well. Second, the impact of these factors on the direct LAP-in-snow albedo reduction varies depending on the LAP concentration. For example, 10 ng/g BC can reduce the broadband albedo of new snow and old snow (snow grain radius of 100 and 1000 μm) by 0.004 and 0.01, respectively; the difference in albedo reduction between these snow types for a given BC concentration is 0.006. For the same snowpack, but with 100 ng/g BC, the difference in albedo reduction between old and new snow is much larger: 0.04 [Dang *et al.*, 2015]. Thus, a shift in grain size does not lead to a fixed albedo reduction with different LAP concentrations. Therefore, uncertainties in the effects of these factors need to be considered in conjunction with uncertainties in the concentrations of LAPs in snow.

Besides the direct radiative forcing, a large fraction of LAP-in-snow radiative forcing results from feedback processes involving both snow metamorphism and atmosphere-snow interactions [Flanner *et al.*, 2007; Bond *et al.*, 2013]. For example, as snow starts to melt, LAPs tend to accumulate at the surface: this further enhances albedo reduction, accelerating snowmelt—a positive feedback process [Doherty *et al.*, 2013]. Such feedback processes cannot be quantified by current observational data, but they are triggered by the direct albedo reduction caused by LAPs in snow; thus, it is crucial to have an accurate estimate of the initial direct albedo reduction in order to calculate both LAP-in-snow direct radiative forcing and adjusted radiative forcing via feedback.

The dependence of BC-in-snow albedo reduction and radiative forcing on different factors has been studied by climate models over different regions. For example, Flanner *et al.* [2007] simulated the impact of snow aging rate, snowmelt-scavenging rate, BC optical properties, snow cover fraction, and BC emissions on BC-in-snow albedo reduction globally and concluded that BC emissions are the largest source of uncertainty. Qian *et al.* [2014] simulated the sensitivity of BC-in-snow albedo reduction to snow aging rate and snowmelt-scavenging ratio over China and the Arctic; their simulated BC mixing ratios agree with the observed BC within a factor of 10. He *et al.* [2014] examined the impact of snow grain shape and BC-in-snow mixing state on BC-snow-radiative forcing over the Tibetan Plateau. These studies provide insightful information toward a better simulation on BC-in-snow albedo reduction, but it is unclear if their results are impacted by biases in the modeled BC concentration.

In this work, we aim to minimize the uncertainty associated with the mixing ratio of BC in snow by using observational data from field campaigns to derive the direct albedo reduction caused by LAPs and BC, and then to quantify the impact of various factors on albedo reduction. The results will also provide insight on what factors should be considered when testing modeled direct radiative effect by LAPs in snow and what processes must be included in models for accurate calculations of radiative forcing.

2. Data and Methods

2.1. Field Observations

2.1.1. Large-Area Field Observations of LAPs in Snow

As stated in section 1, our group and collaborators have carried out several large-area field campaigns in the Arctic, China, and North America. The Arctic survey expanded the first survey carried out by Clarke and Noone in 1983–1984 [Clarke and Noone, 1985] and reported the concentration of LAPs in snow from fieldwork done in 1998 and the years 2005–2009 across a much larger region in the Arctic including the Arctic Ocean, Greenland, Canada, and Siberia [Doherty *et al.*, 2010]. In January and February of 2010, a similar large-area survey was conducted to study the snow in north-central and northeastern China [Huang *et al.*, 2011; Wang *et al.*, 2013]. This was the first large-area survey of LAPs in snow conducted in the midlatitude Northern Hemisphere. The same research team then carried out a similar field campaign 2 years later to sample snow in Northwestern China [Ye *et al.*, 2012]. In the winter of 2013, the first large-area field campaign on LAPs in snow in North America was conducted across 13 states in the U.S. and three provinces in Canada [Doherty *et al.*, 2014]. In the winter of 2014, samples were collected at three fixed sampling locations in Idaho over a period of about 2 months [Doherty *et al.*, 2016]. In this work, we focus only on the large-area surveys reported by Doherty *et al.* [2010] (Arctic survey), Wang *et al.* [2013] (north China survey), and Doherty *et al.* [2014] (North America survey).

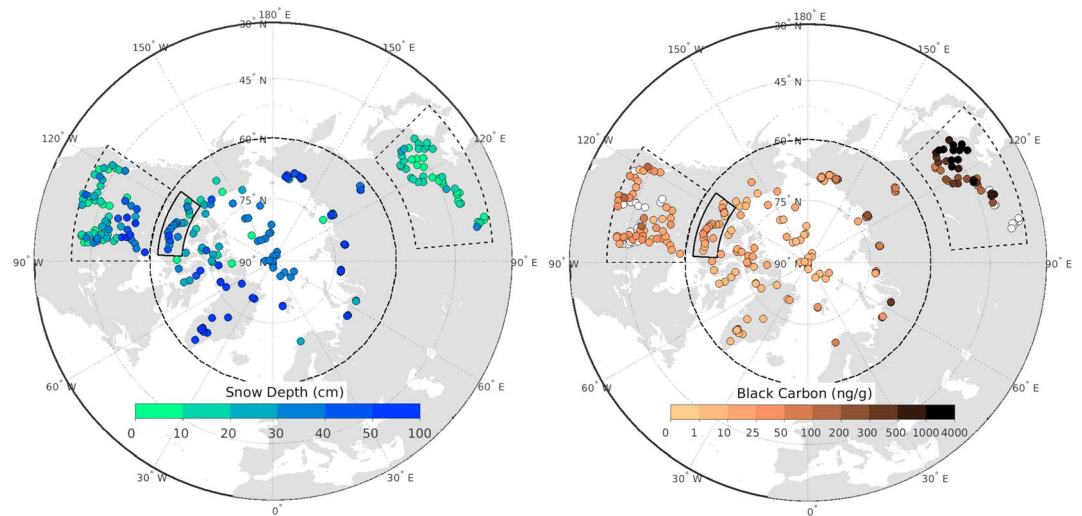


Figure 1. Snow depth and black carbon concentration (top 5 cm) at sampling locations. Sites are grouped into three major regions by dashed lines: North America (January–March 2013 [Doherty et al., 2014]), Arctic (spring and summer, 1998, 2005–2009 [Doherty et al., 2010]), and China (January–February 2010 [Wang et al., 2013]). Sampling sites in subarctic Canada with additional snow depth data are enclosed with black solid lines [Sturm et al., 2008]. The white dots show sites where BC concentration was indeterminate because of high dust content.

The snow samples were mostly collected in seasons when the snowpack was near its maximum depth and before the snow started to melt. The samples in the midlatitudes were collected in late winter and early spring, while the samples in the Arctic were collected across multiple months in spring and summer. Sampling locations were far from major roads and populated areas to avoid local contamination. The snowpacks at these sampling sites generally represented the snow in surrounding areas. At each sampling site a snow pit was dug and two vertical profiles obtained: snow samples were collected for multiple layers depending on the snow stratigraphy. The collected snow samples were then melted and passed through filters. Filters loaded with particles from the snow were measured using a spectrophotometer to estimate the concentration of BC and non-BC LAPs in the snow. The detailed procedures on snow collection and filtration can be found in Doherty et al. [2010] and Doherty et al. [2014], and the description of photometer and optical methods can be found in Grenfell et al. [2011] and Doherty et al. [2010]. In this work, we will mainly use the following data acquired from these field expeditions:

1. Snow depth (cm)
2. Snow density (kg/m^3) profile
3. C_{LAP} (ng/g) profile: equivalent amount of BC if all light absorption by particles in snow was due to BC. This quantity is given as $C_{\text{BC}}^{\text{equiv}}$ in the studies cited above.
4. C_{BC} (ng/g) profile: estimated concentration of BC in snow. This quantity is given as $C_{\text{BC}}^{\text{est}}$ in the studies cited above.
5. C_{NBC} (ng/g) profile: equivalent amount of BC that would be needed to explain the absorption by non-BC LAPs. $C_{\text{NBC}} = C_{\text{LAP}} - C_{\text{BC}}$.

Using this optical technique, absorption by LAPs and non-BC LAPs are converted into the equivalent mass of BC that would be needed to produce the same amount of absorption [Grenfell et al., 2011]. Therefore, although we do not know the concentration and optical properties of non-BC LAPs, we can still derive their impact on snow albedo as long as we know the optical properties of BC. This allows us to calculate snow albedo reductions due to both BC and non-BC constituents, as described in section 2.3.1.

The snow depth and BC concentration in the top 5-cm snow layer at all sampling sites are shown in Figure 1. In the Arctic and North America, snow is deeper and contains lower concentrations of BC, while in China, the snow is shallower and contains larger concentrations of BC. In Figure 2 we show the regional variations of these two quantities for the three regions outlined by dashed lines in Figure 1. For the Arctic, North America, and China, the mean snow depths are 38, 26, and 14 cm, respectively, and the mean BC

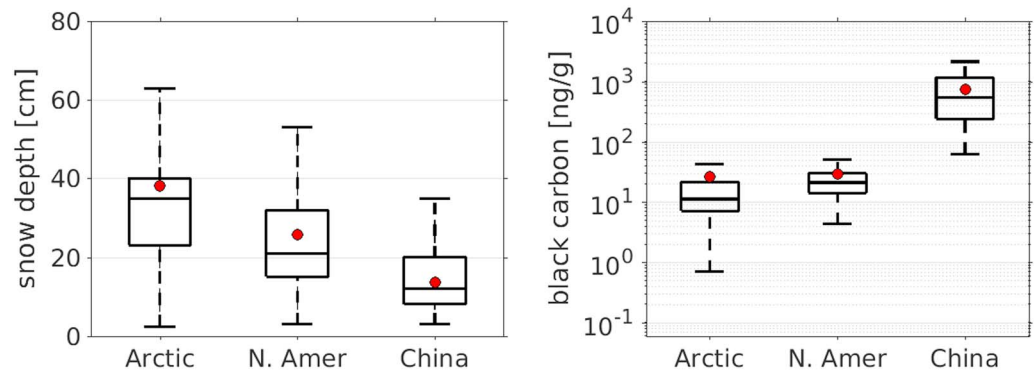


Figure 2. Site-averaged snow depth and black carbon concentration (top 5 cm) in three regions: mean (dot), median (bar), 25th and 75th percentiles (box), and maximum/minimum values within ± 2.7 standard deviation (whiskers). The setup for the following box-whisker plots is the same.

concentrations of surface layer are 27, 29, and 760 ng/g, respectively. The range of BC mixing ratios in China is large. As described previously, it is important to note that these snow samples were collected at the end of snowy season of different years at different locations. If the interannual variability of snow amount and aerosol emissions is large at the sampling sites, the results may be unrepresentative.

2.1.2. Snow Depth Distribution in Subarctic Canada

In Figure 1, 22 snow sampling sites in subarctic Canada are grouped and boxed by a solid line. Snow samples at these sites were collected during April of 2007 as part of a snow survey [Sturm *et al.*, 2008]. In addition to collecting snow samples at a given location, they also measured the snow-depth distribution in the surrounding area. At each sampling location, up to 600 distributed snow depths were reported [see Sturm *et al.*, 2008, Appendix B]. We do not have snow-depth distributions in other regions, so we will use this unique data set to illustrate the impact of depth distribution on snow albedo, following the methods described in section 2.3.2.

2.2. Albedo Calculation

2.2.1. Single-Scattering Properties of Ice and BC

The single-scattering properties of ice and BC are calculated using Mie theory with optical constants of ice from Warren and Brandt [2008] and optical constants of BC from Bond and Bergstrom [2006]. Following Dang *et al.* [2015, 2016], the complex refractive index of BC is $m = 1.95 - 0.79i$, independent of wavelength, and the density of BC is 1.8 g cm^{-3} [Bond and Bergstrom, 2006]. We assume BC has a lognormal size distribution of geometric width 1.3 and mass mean diameter $0.13 \text{ }\mu\text{m}$ [Clarke *et al.*, 1987]. The mass absorption cross section (mass absorption efficiency) of BC is therefore $6.73 \text{ m}^2/\text{g}$ at wavelength $550 \text{ }\mu\text{m}$. We assume that the snow grains are spherical with radii of either $100 \text{ }\mu\text{m}$ or $1000 \text{ }\mu\text{m}$, which correspond to the typical effective grain radii of new snow and old melting snow, respectively [Wiscombe and Warren, 1980]. The asymmetry factor of snow grains would be different if the grains were nonspherical. The impacts of snow grain shape on snow albedo and the albedo reduction by BC have been examined by Dang *et al.* [2016]. They found that these effects can be mimicked by using a smaller grain of spherical shape in radiative transfer calculations. In this work, we adopt the spherical assumption because we select effective snow radii that were derived from comparisons between radiative transfer calculations and measurements [Wiscombe and Warren, 1980; Grenfell *et al.*, 1994]; thus, the impact of snow grain shape on snow albedo has already been included. For snowpacks containing BC, we assume that BC particles and ice particles are externally mixed, i.e., the single-scattering properties of snowpacks are the cross-section-area-weighted sum of the single-scattering properties of BC and ice separately [Dang *et al.*, 2015].

2.2.2. Spectral Albedo

The single-scattering quantities of snow are put into a radiative transfer model to calculate the spectral albedo, α_{λ} , of snowpacks using the discrete ordinates method [Stamnes *et al.*, 1988] for wavelengths of 0.2 to $4 \text{ }\mu\text{m}$. For all calculations, we use a solar zenith angle of 49.5° with a cosine of 0.65. This is the effective solar zenith cosine for diffuse radiation under a cloud; it is close to the insolation-weighted solar zenith cosine for the sunlit hemisphere (0.66), and it may also allow us to estimate the albedo for other solar zenith angles by altering the effective snow grain radius [Marshall, 1989], as discussed by Dang *et al.* [2015].

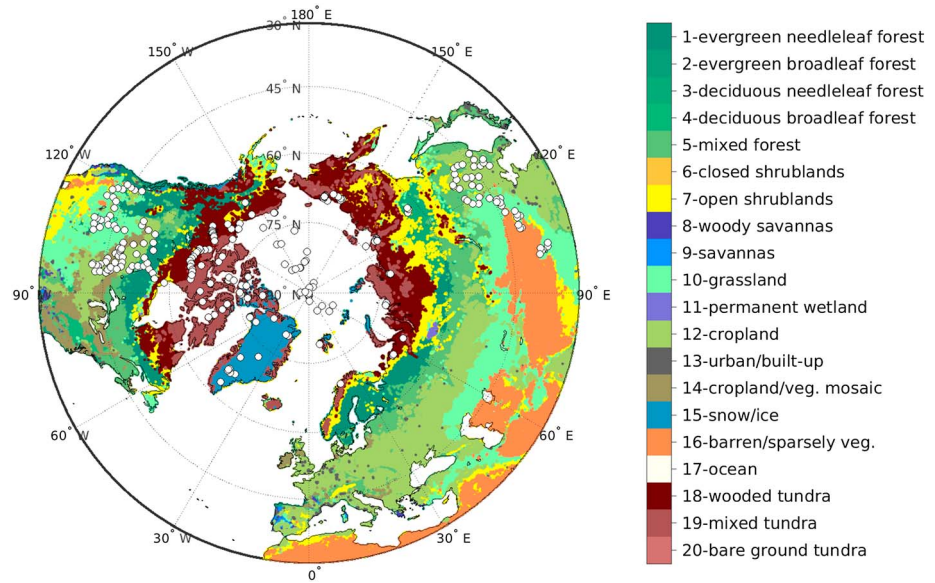


Figure 3. Surface types at snow-sampling locations (NOAHv3.3 vegetation data set, <http://ldas.gsfc.nasa.gov/gldas/GLDASvegetation.php>).

For an optically thin snowpack, the albedo of the underlying ground is also important because the ground can absorb light that penetrates through the snowpack. The albedo of the underlying ground depends on the location and time of year. As shown in Figure 3, in the midlatitude regions we sampled, the underlying ground for most snow-sampling locations is short grass. In subarctic Canada and Russia, the underlying ground is usually tundra or damp soil. In Greenland and on the Arctic Ocean, what is beneath snow is ice sheet and sea ice, respectively. Based on the location of the snow sampling sites, we use the spectral albedo of different surface types, as shown in Figure 4. These data were measured by different groups [Liang *et al.*, 2002; Brandt *et al.*, 2005; Bøggild *et al.*, 2010] and then extrapolated to 0.3 to 4 μm for computational use. For each snow sampling site, we use the appropriate ground albedo for the radiative transfer calculation: China

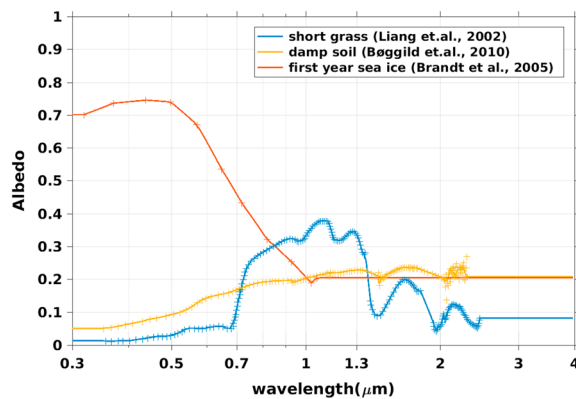


Figure 4. Spectral albedo of grassland, soil, and sea ice. Albedo of grassland was measured in Maryland [Liang *et al.*, 2002, Figure 3]; albedo of damp soil was measured on bare ground tundra of northeast Greenland [Bøggild *et al.*, 2010, Figure 6]; albedo of first-year sea ice was measured on the Antarctic Ocean [Brandt *et al.*, 2005, Figure 1]. The extrapolations of measured albedo (plus marks) to shorter and longer wavelengths (0.3–4 μm) are illustrated by the solid lines.

and North America (grassland), subarctic and arctic Canada and Russia (damp soil), and Arctic Ocean (first year sea ice); for Greenland, there is no need to specify the underlying surface because the observed snow depth on the ice sheet is effectively semi-infinite.

Snow grain size was also estimated visually with a magnifying glass in many of the snow pits. However, we do not use those grain sizes in our calculations because our aim is not to compute the albedo at the exact moment of sampling. The grain sizes we find at the surface are the result of temperature and time since snowfall and can be altered by wind, so we do not take them to be representative of that location over a month or

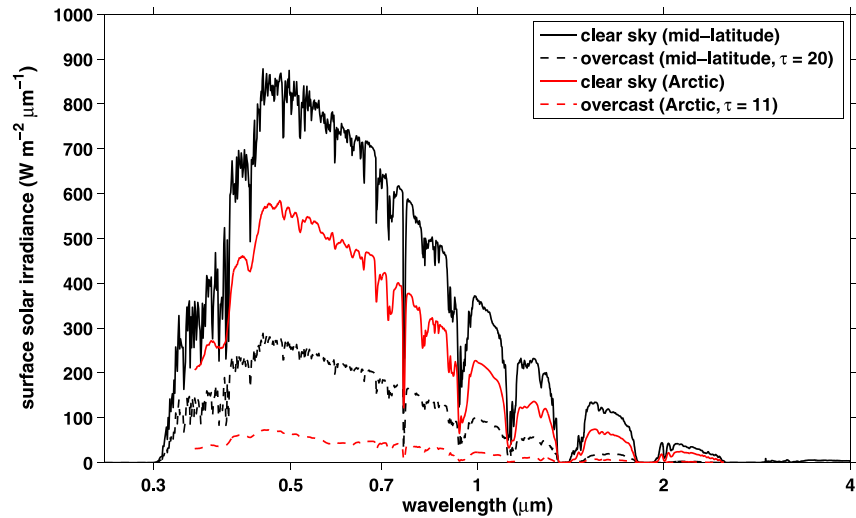


Figure 5. Incident solar spectra used for broadband albedo calculation. The spectra for Northern Hemisphere midlatitude are calculated using atmospheric model SBDART with standard atmospheric profiles for winter. The spectra for Arctic were measured at the Arctic Ocean in summer by Grenfell and Perovich [2008].

season. Instead, we perform albedo computations for two idealized snow grain sizes representing fine-grained new snow and coarse-grained old melting snow, which effectively are bounding limits. Thus, although the snow was sampled before melting began (snow grain size likely closer to 100 μm), we also compute what the albedo will be at that location when the snow is melting later in the spring (snow grain size likely closer to 1000 μm).

2.2.3. Broadband Albedo

The spectral albedo, α_λ , of snowpacks is integrated over the solar spectrum ($\lambda = 0.2$ to $4 \mu\text{m}$) and weighted by the incoming solar irradiance $S(\lambda)$ to calculate broadband albedo α .

$$\alpha = \frac{\int \alpha_\lambda S(\lambda) d\lambda}{\int S(\lambda) d\lambda}$$

For snow sampling sites in the Arctic, we use the incoming solar spectra measured at the Arctic sea surface by Grenfell and Perovich [2008]. This measurement covered the wavelength range of 0.35–2.5 μm and was extended to 0.2–4 μm by use of the atmospheric model SBDART [Ricchiuzzi et al., 1998] for the subarctic summer standard atmosphere. The spectra measured under cloudy sky can be matched by specifying a cloud optical depth of 11 in SBDART. For snow sampling sites in China and North America, we use the surface solar spectra calculated by SBDART for the midlatitude winter standard atmosphere, where the cloud optical depth of cloudy sky is set to 20. These solar spectra are shown in Figure 5. Clear-sky albedo and cloudy-sky albedo are calculated separately using the corresponding spectra. The all-sky albedo is the weighted average of clear-sky albedo and cloudy-sky albedo, depending on the cloud fraction (CF, %, as shown in Figure 6).

$$\alpha_{\text{all sky}} = \text{CF} * \alpha_{\text{cloudy sky}} + (1 - \text{CF}) * \alpha_{\text{clear sky}}$$

In midlatitudes, depending on the specific location, snow starts to melt between mid-February and mid-March, so to calculate the all-sky albedo of snowpacks in this region, we apply cloud fraction of February for new snow ($r = 100 \mu\text{m}$) and of March for old-melting snow ($r = 1000 \mu\text{m}$). At higher latitudes, snow starts to melt later; we therefore use the cloud fraction of March for new snow ($r = 100 \mu\text{m}$) and of April for old-melting snow ($r = 1000 \mu\text{m}$) to calculate the all-sky albedo of snowpacks in this region. If not noted otherwise, the albedos given in this paper are all-sky broadband albedo calculated using the cloud fraction shown in Figure 6.

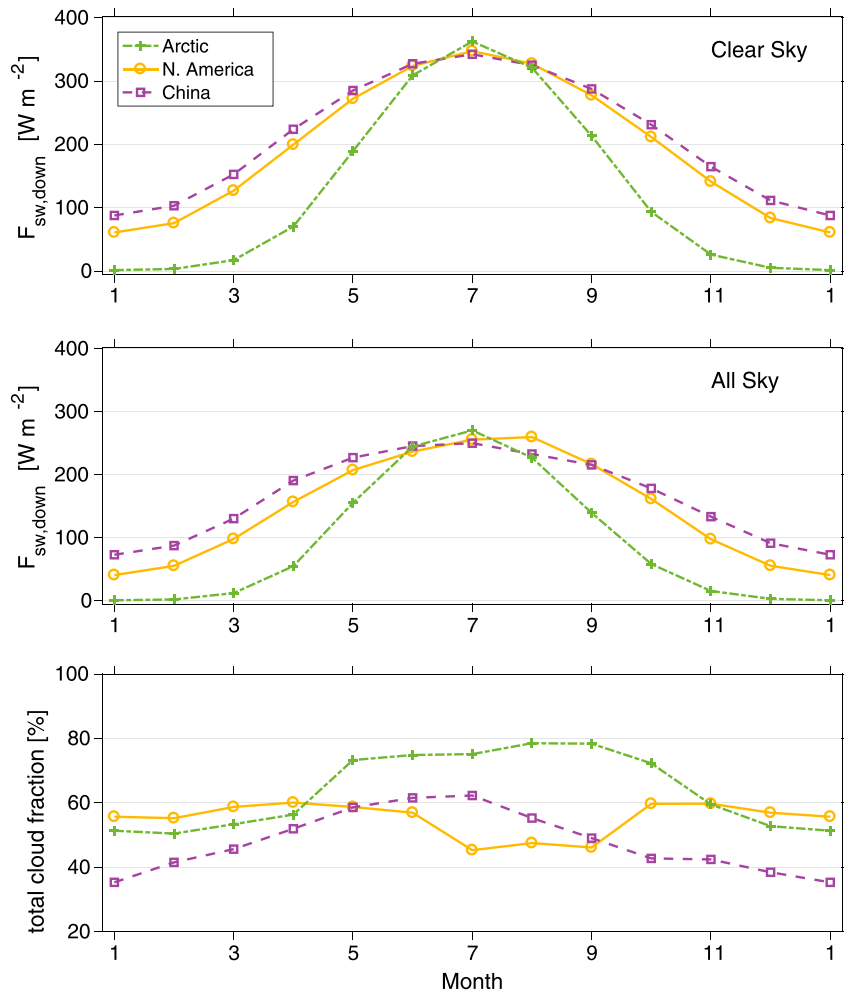


Figure 6. (top and middle) Monthly mean downward surface shortwave flux (clear sky and all sky) and (bottom) total cloud fraction (sum of low, middle, and high clouds during daytime) in three sampling regions. The flux and cloud cover data are obtained from CERES (<https://ceres.larc.nasa.gov/products.php?product=SYN1deg>).

2.2.4. BC-in-Snow Radiative Forcing

Direct radiative forcing by BC in snow is estimated by multiplying the derived albedo reduction by the downward shortwave flux at surface. As shown in Figure 6, both solar flux and cloud fraction are acquired from the CERES (Clouds and the Earth’s Radiant Energy System) [Wielicki *et al.*, 1996] product “CERES SYN1deg” (<https://ceres.larc.nasa.gov/products.php?product=SYN1deg>). The downloaded 3 h data are first averaged over 10 years from 2005 to 2014, then averaged over three separate regions defined in Figure 1. As was done for the calculation of all-sky albedo, we use fluxes of different months for midlatitudes and high latitudes as well.

2.3. Computation Scenarios

Combining observational data sets with a radiative transfer model enables us to calculate snow albedo for different scenarios to (1) quantify the albedo reduction by light-absorbing particles and (2) explore the impact of different factors on derived albedo reduction by BC.

2.3.1. LAPs

Using the observed snow depth and snow density profile, we can calculate the albedo of snowpacks containing different types of LAPs, specifically for the following four scenarios:

1. Pure: snow does not contain any LAPs.
2. BC: snow contains only BC, with concentration C_{BC} .

3. Non-BC: snow contains only non-BC LAPs (here we use snow containing the “equivalent” BC, with concentration C_{NBC}).
4. LAPs: snow contains both BC and non-BC LAPs (we use the concentration C_{LAP} ; the albedo calculated in this scenario reflects the true LAP composition of the sampled snowpack).

By taking the differences in snow albedo between pure snow and snow containing different LAPs, we can derive the albedo reduction by different types of LAPs. The results are discussed in section 3.1.

2.3.2. Vertical Profiles

In the field, snow samples were collected from layers from the top to the bottom of snowpack, so we have vertically resolved concentrations of BC and non-BC LAPs. The number of layers varies depending on snow depth and stratigraphy; the number of layers sampled was typically 5; the maximum was 24, in Greenland. In this work, we therefore use a multilayer radiative transfer model to compute the albedo of snowpacks with no restriction on the number of layers. However, this may not be an option for climate models. To examine the impact of vertical profiles on snow albedo and albedo reduction by BC, we compute the snow albedo for the following four scenarios:

1. *Multi-layer*: multilayer snowpacks. Snow density and mixing ratio of LAPs are vertically resolved based on field observations. The albedo calculated in this scenario is used as the reference calculation for the sampled snowpacks (given the specified grain size).
2. *One-layer (column-mean BC)*: one-layer snowpack. Snow density and mixing ratio of LAPs are the snow mass-weighted average of the entire snowpack, based on the profiles from field observations.
3. *One-layer (top 5 cm mean BC)*: one-layer snowpack. Snow density and mixing ratio of LAPs are the values measured in the top 5 cm of snowpacks. For this case, the column-integrated BC mass is different from observations.
4. *Two-layer*: two-layer snowpack. The top layer is 5 cm and the subsurface layer is the entire snow column below the top 5 cm. Snow density and mixing ratio of LAPs in these two layers are the snow mass-weighted average of samples from within the top 5 cm and lower layers, respectively.

For a specific snow-sampling site, the column-integrated snow mass and LAP mass are the same in scenarios (1), (2), and (4). The results are discussed in section 3.2.

2.3.3. Sensitivity Tests on BC Concentration and Snow Depth

As discussed in the introduction, model-simulated BC concentrations agree with observations only to within a factor of 10. In addition, model simulation of snow depth is also subject to large uncertainty. For a given snow grain radius, the albedo reduction by BC is mostly determined by the amount of BC and the snow depth (if the snow is thin). Therefore, it is important to evaluate the uncertainty/bias in BC-in-snow albedo reduction caused by the uncertainty/bias in both BC concentration and snow depth. For these sensitivity tests, we decrease/increase the observed BC concentration and snow depth by dividing/multiplying by factors of 2, 5, and 10 and evaluate the changes in computed BC-in-snow albedo reduction. If the adjusted snow depth is shallower than what was observed, we only consider the top snow layers within the adjusted snow depth. For example, if the sample snowpack was 20 cm deep, the adjusted snow depth is 4 cm if we divide the original depth by a factor of 5; in this case, we remove the bottom 16 cm of snow and calculate the snow albedo as if the snow were only 4 cm deep. If the adjusted snow depth is deeper than what was observed, we extend the bottom layer to match the target depth, with same black carbon concentration. To evaluate the maximum potential impact of BC-in-snow, we also included one more case by setting the snow depth to 100 m (optically deep snow). The albedo calculated in this scenario will illustrate the BC-induced snow albedo reduction if all sampling snowpacks were optically semi-infinite. For the sensitivity tests, the snow-column-integrated black carbon mass differs from the observed values. The results are discussed in section 3.3.

2.3.4. Snow Depth Distribution

Using field data described in section 2.1.2, we will show the impact of snow-depth distribution on snow albedo and BC-in-snow albedo reduction. At each sampling site, albedo and albedo reduction by BC is calculated both for the mean snow depth and for a distribution of snow depths from the field measurements in subarctic Canada. In our calculation, the concentrations of light-absorbing particles and the snow density are the same for each of the numerous depth-measurements made at the site. The resulting difference in snow albedo or albedo reduction by BC is therefore due only to depth distribution. These results are discussed in section 3.4.

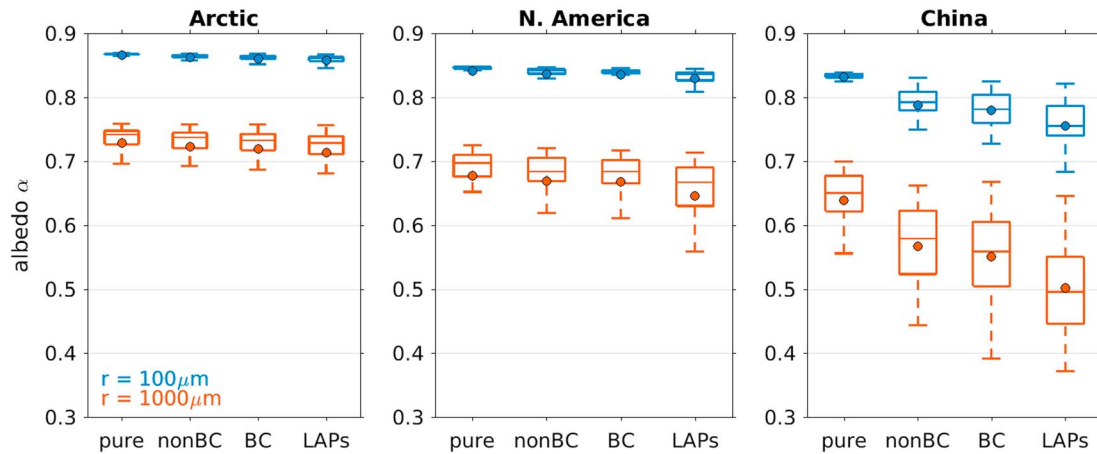


Figure 7. All-sky broadband albedo of snow derived from observational data sets for three regions. In each region, albedo is calculated for new snow ($r = 100 \mu\text{m}$) and old-melting snow ($r = 1000 \mu\text{m}$), and for four scenarios described in section 2.3.1: (1) pure: snow does not contain any LAPs; (2) nonBC: snow contains non-BC LAPs only; (3) BC: snow contains BC only; (4) LAPs: snow contains both BC and non-BC LAPs. Figure convention: mean (dot), median (bar), 25th and 75th percentiles (box), and maximum/minimum values within ± 2.7 standard deviation (whiskers).

In the result section, we will derive and discuss the following quantities:

1. α : all-sky broadband albedo of snowpacks;
2. $\Delta\alpha$: reduction of α induced by different LAPs in snow;
3. $\delta\alpha$ and $\delta\Delta\alpha$: change in α or $\Delta\alpha$ if snow conditions, LAPs concentrations, or model setup change.

2.4. Calculation of Regional Data

In the Results section, we will mainly discuss the averaged results in each region or regional variation. Generally, at each snow-sampling site, we perform radiative transfer calculations on one snowpack with the observed profiles and then with modified profiles, depending on the scenario. For each scenario, we then calculate the regionally averaged results by averaging across all sites within a given region. At some sites, the concentration of non-BC particles is so high that the estimated BC concentration is no longer accurate (see *Doherty et al. [2010, Figure 16]*, and associated discussion); we excluded these sites when quantifying the impact of BC on snow. For this reason, although snow samples were collected at 46 sites in China and 67 sites in North America, the final number of snow sampling sites used in this work are 37 and 49 for these two regions, respectively. For the Arctic, the number of snow sampling profiles used here is 209. Some of these were snow samples collected at the same location but at different times [*Doherty et al., 2010*]; these samples were considered as individual sites in the statistical analysis.

Table 1. Regional Averages From Observation and Radiative Transfer Calculations^a

		Arctic		North America		China	
		$r = 100 \mu\text{m}$ (March)	$r = 1000 \mu\text{m}$ (April)	$r = 100 \mu\text{m}$ (February)	$r = 1000 \mu\text{m}$ (March)	$r = 100 \mu\text{m}$ (February)	$r = 1000 \mu\text{m}$ (March)
Snow depth	(cm)	38		26		14	
Black carbon BC (top 5 cm)	(ng/g)	27		29		760	
Black carbon BC (subsurface)	(ng/g)	21		30		480	
Snow albedo		0.86	0.71	0.83	0.65	0.76	0.50
Albedo reduction by BC	(10^{-4})	45	87	48	86	314	578
Albedo reduction by all LAPs	(10^{-4})	85	153	116	196	773	1379
Cloud cover	(%)	53	56	55	59	42	46
Downward shortwave flux F_{sw}	(W m^{-2})	12	55	56	98	88	130
Shortwave forcing by BC	(W m^{-2})	0.06	0.5	0.3	0.8	2.8	7.5

^aThe snow albedo and albedo reduction for the all-sky case are calculated based on the monthly-averaged cloud fraction in different regions.

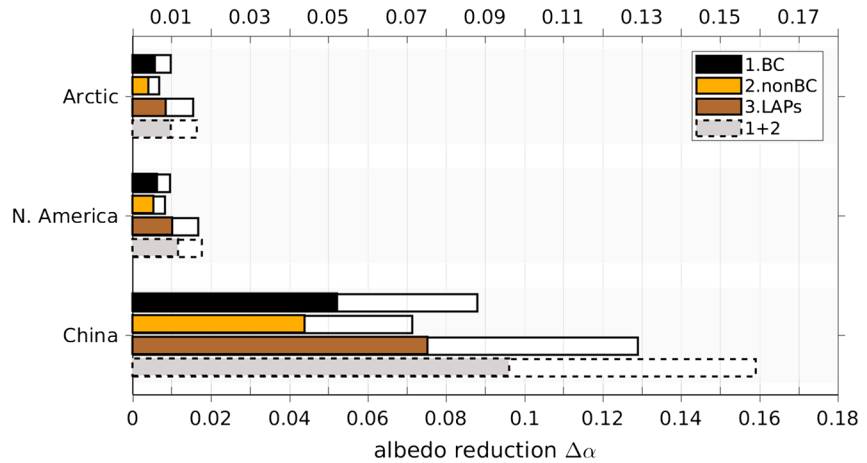


Figure 8. Regional-averaged broadband albedo reductions (all-sky) induced by different LAPs for new snow (color-filled bars) and for old-melting snow (extended white bars). The black, yellow, and brown bars denote the albedo reductions by BC, non-BC LAPs, and all LAPs (BC + non-BC LAPs) compared with the albedo of pure snow. The grey bars are the sum of albedo reductions caused by BC and non-BC separately.

3. Results

3.1. Snow Albedo and Albedo Reduction Induced by Black Carbon (BC)

Albedos of snowpacks containing different types of LAPs are shown in Figure 7, and the regional means are given in Table 1. The regional variation of snow albedo in China is much larger than that in the Arctic and North America. The climate-model simulations for snow albedo in China therefore should use a finer geographical resolution.

Albedo reductions by BC, non-BC LAPs, and total LAPs are shown in Figure 8. For new snow containing BC only, the albedo reductions caused by BC are 0.006, 0.006, and 0.052 in the Arctic, North America, and China, respectively. For snow containing non-BC LAPs only, the albedo reduction caused by non-BC LAPs is slightly smaller than the albedo reduction caused by BC but of the same order of magnitude. The albedo reductions caused by all LAPs are 0.009, 0.012, and 0.077 in the Arctic, North America, and China. These values

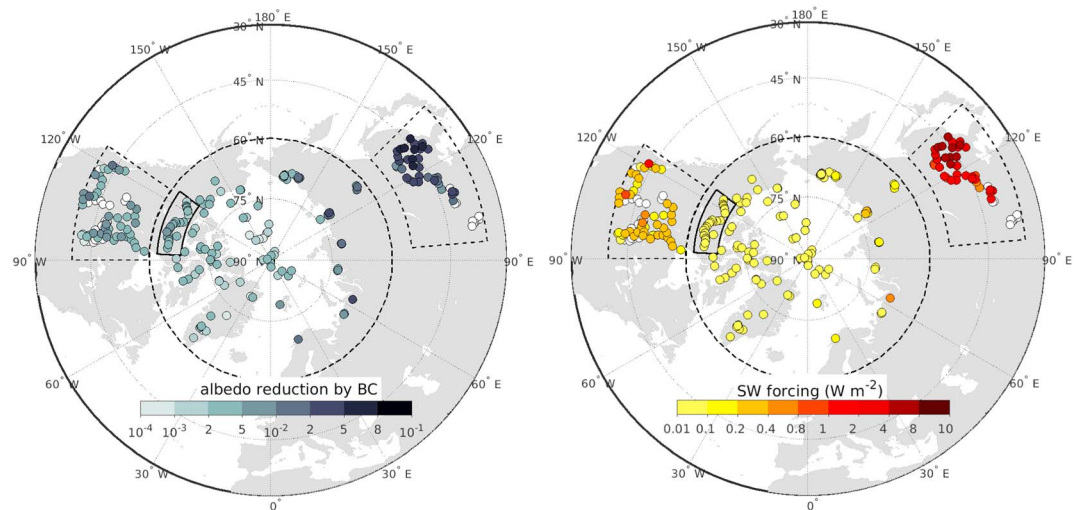


Figure 9. All-sky direct albedo reduction and radiative forcing induced by BC in snow (new snow, $r = 100 \mu\text{m}$) for February (North America and China) and March (the Arctic). The white dots show sites with indeterminate BC concentrations, and therefore, no estimation of albedo reduction and radiative forcing are made for those sites.

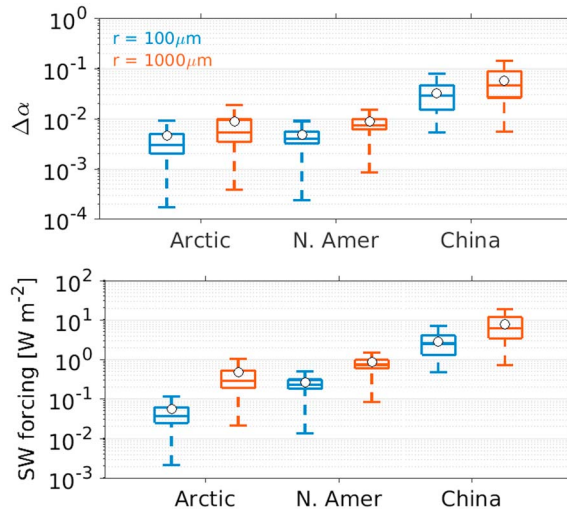


Figure 10. All-sky direct albedo reduction and radiative forcing induced by BC in snow in three regions. For new snow ($r = 100 \mu\text{m}$), cloud cover and shortwave flux of February and March are used for midlatitudes and high latitudes, respectively, while for old snow ($r = 1000 \mu\text{m}$), values of March and April are used for midlatitudes and high latitudes, respectively. Figure convention: mean (dot), median (bar), 25th and 75th percentiles (box), and maximum/minimum values within ± 2.7 standard deviation (whiskers).

are smaller than the sum of albedo reductions caused by BC and non-BC LAPs separately. This is because the penetration depth of light decreases as the concentration of LAPs increases, so albedo reduction does not increase linearly with the addition of LAPs.

There are significant amounts of non-BC LAPs emitted from natural sources (e.g., desert dust), and these are present in snow regardless of human activities, in some locations in high concentrations. Thus, natural snowpacks are not pure, and baseline calculations of the albedo of non-polluted snow for radiative forcing calculations must account for this. To evaluate the impact of anthropogenic BC on snow albedo, or to quantify the radiative forcing induced by BC, we need to study the impact of

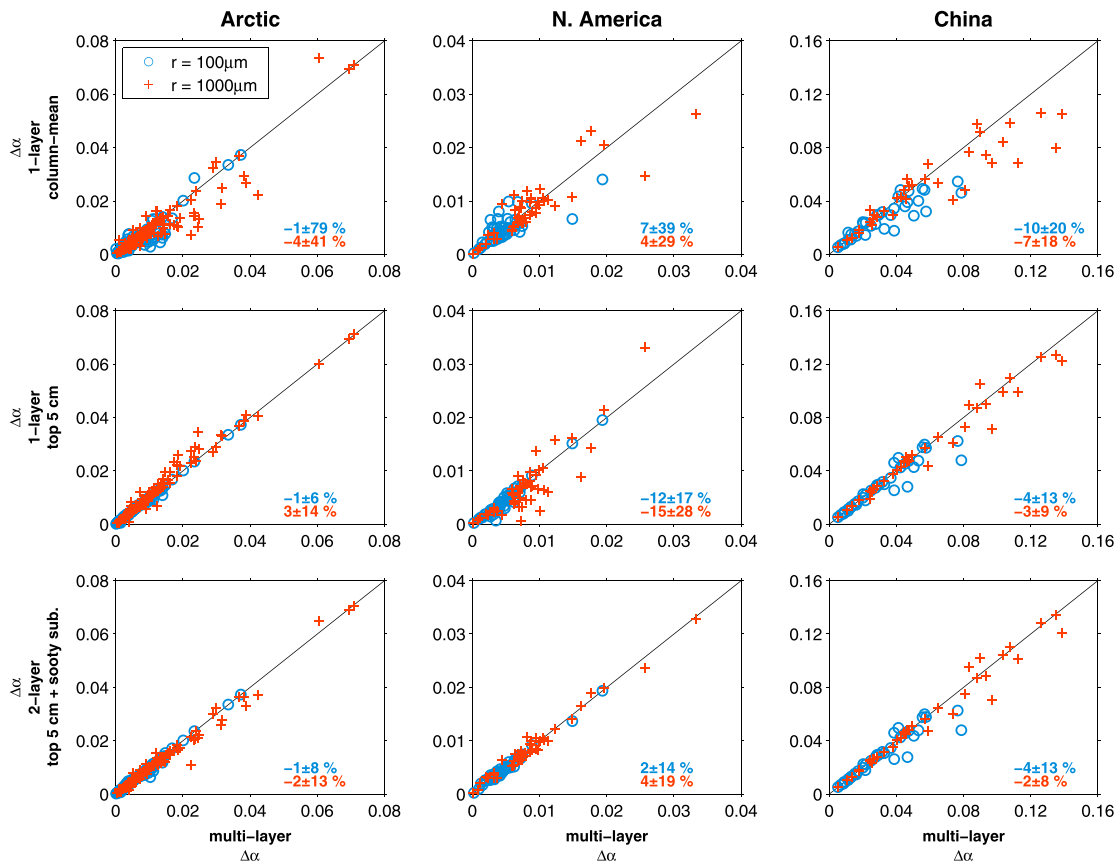


Figure 11. Comparison of direct albedo reduction (all-sky) induced by BC calculated with three vertical resolutions: multilayer, one-layer, and two-layer snowpacks as described in section 2.3.2, for new snow ($r = 100 \mu\text{m}$) and old snow ($r = 1000 \mu\text{m}$). Numbers shown in the bottom right of each figure are the percentage errors and standard deviations of calculated albedo reduction if the vertical profiles of BC concentration were changed.

BC on snowpacks that already contain natural, non-BC LAPs. If snow already contains the observed amounts of non-BC LAPs, the albedo reductions caused by BC are 0.005, 0.005, and 0.031 in the Arctic, North America, and China; these albedo reductions would increase by 30% if the snow did not contain non-BC LAPs. The impacts of LAPs on snow albedo in different scenarios are much larger for old melting snow ($r = 1000 \mu\text{m}$); this is because shortwave radiation penetrates deeper in coarse-grained snow and encounters more of the LAPs. These regional averaged data are illustrated in Figure 8 and also listed in Table 1.

The BC-in-snow albedo reduction and direct radiative forcing are derived and shown in Figure 9 (for new snow only) and in Figure 10. These are the forcings that apply where snow is present; the regionally averaged forcing would need to account for fractional snow cover, which we do not consider here. Note that this forcing does not include any feedback, e.g., to snow grain size or snowmelt, so will be smaller than if they did include these feedbacks, as in some previous forcing calculations [e.g., *Flanner et al.*, 2009; *Bond et al.*, 2013]. In the Arctic and North America, the albedo reductions caused by BC are similar: 0.005 and 0.009 for new snow and old snow, respectively, in both regions. Despite the similar albedo reduction, the radiative forcing by BC in snow in North America is much larger because the solar insolation is much larger at midlatitudes than at high latitudes (Figure 6). The albedo reduction caused by BC in China is considerably larger than in the other two regions: 0.03 and 0.06 for new snow and old snow. For new snow, the direct radiative forcings by BC are 0.06, 0.3, and 3 W m^{-2} in the Arctic, North America, and China, respectively. For old snow, the direct forcing is much larger: 0.5, 0.8, and 8 W m^{-2} , respectively. This radiative effect includes all BC measured in the snowpack, but it is unclear whether all BC is emitted from anthropogenic sources.

3.2. Impact of Vertical Profiles on Albedo Reduction by Black Carbon (BC)

Figure 11 shows the derived BC-in-snow albedo reduction from radiative transfer calculations using the different vertical profiles described in section 2.3.2. The results of one-layer and two-layer models are compared against the results of the multilayer model. The ranges of errors in albedo reduction derived from the one-layer model with column-mean BC are the largest (Figure 11, top row). These ranges are much reduced if we apply the BC concentration of the surface layer (top 5 cm) to the entire snow column (Figure 11, middle row). If we use a two-layer model that accounts for BC in the lower layer, both mean errors and error ranges are reduced to the minimum, especially for North America (Figure 11, bottom row). Despite these changes in the vertical profiles of snowpack, the resulting albedo reductions in the Arctic are similar. In China, the high concentrations of LAPs mean that light does not penetrate as deeply; the relative impact of BC profiles on derived albedo reduction is therefore also smaller. In North America, the albedo reduction is more sensitive to the profiles of BC concentrations. Overall, a correct concentration of LAPs in the top 5 cm is crucial for determining albedo reductions for all three regions.

3.3. Sensitivity Tests

As discussed in section 3.1, the albedo reduction caused by BC is smaller if the baseline snowpack contains non-BC LAPs than if the baseline snowpack is clean. There are other factors that also influence BC-in-snow albedo reduction. In Figure 12, we show the relative changes in albedo reduction for different snow conditions, cloud cover, and for a range of BC concentrations and snow depths. Absolute changes in albedo reduction are summarized in Table 2. The percentages discussed in this section are absolute changes of albedo reduction induced by BC (blue-shaded columns in Table 2).

We first consider the case of new snow with observed BC concentrations (Figure 12a). If the snowpack is optically thick and does not contain non-BC LAPs in addition to the BC (x-label case “deep, BC only”), the albedo reduction by BC increases in all three regions by a factor of 2 for new snow (and by a factor of 3–6 for old melting snow) relative to the case where the observed snow depth is used. Similarly, the albedo reduction by BC also increases if snow depth is optically thick (x-label case “deep”) or if the snow depth is as-observed but does not contain non-BC LAPs (x-label case “BC only”). In the Arctic and North America, if the new snow were optically thick, the albedo reduction induced by BC would increase by 20–50%. If non-BC LAPs were not present in the snowpack, the albedo reduction induced by BC would increase by ~30% in the Arctic and North America and by 70% in China. The relative change is larger for old snow than for new snow in all three regions.

The spectral solar irradiance under cloudy sky is richer in visible wavelengths because clouds filter out the near-IR wavelengths. The broadband albedo reduction caused by BC is therefore larger under cloudy sky

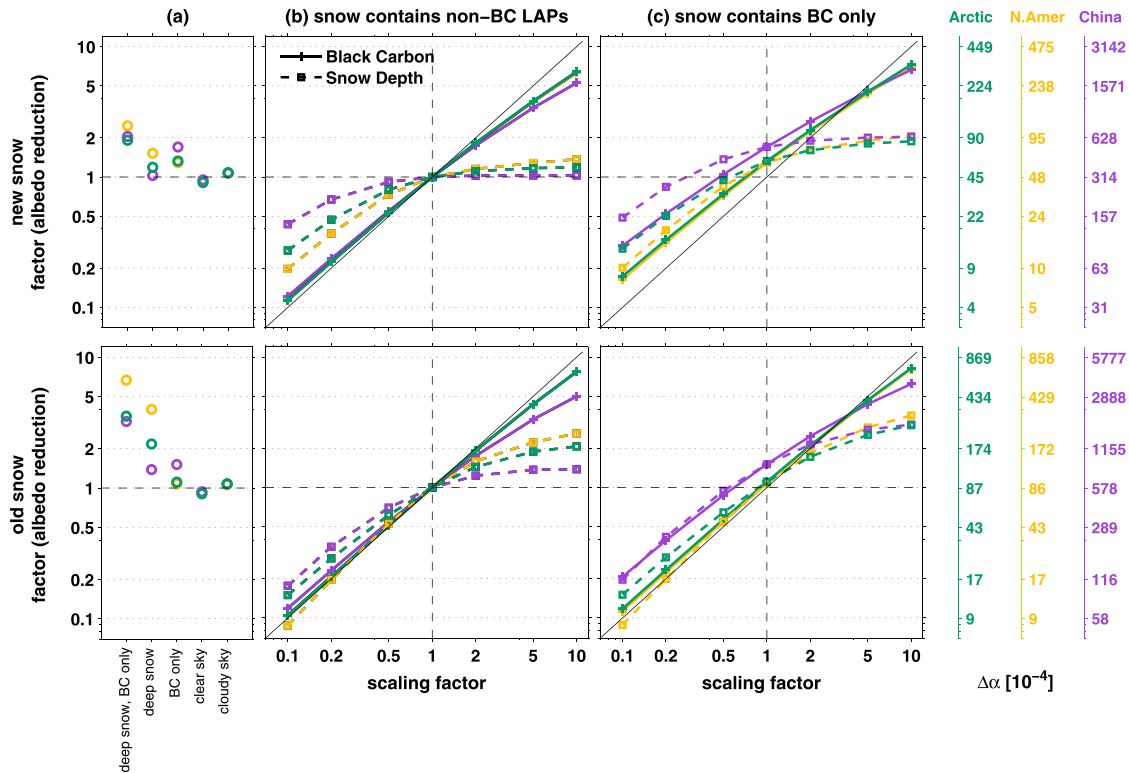


Figure 12. Relative change in BC-in-snow albedo reduction (left axis, $\Delta\alpha_{5T}/\Delta\alpha$) resulting from varying different parameters in the cases of new snow ($r = 100 \mu\text{m}$) and old snow ($r = 1000 \mu\text{m}$). The values of $\Delta\alpha$ (right axes) and $\Delta\alpha_{5T}$ used in this calculation are BC-in-snow albedo reductions calculated with observed data (snowpacks containing both BC and non-BC LAPs with observed snow depth) and using adjusted parameters, respectively. (a) One or more conditions are altered as labeled on the x axis. From left to right, these are (1) deep snow, BC only: increasing snow depth to optically thick and removing non-BC LAPs; (2) deep snow: optically thick snow; (3) BC only: removing non-BC LAPs such that snow contains only BC; (4) clear sky; and (5) cloudy sky. In the center and right panels, the BC concentration and snow depth are scaled by factors of 0.1, 0.2, 0.5, 2, 5, and 10 for models that (b) include non-BC LAPs or (c) do not include non-BC LAPs.

(x-label case “cloudy”) than under clear sky (x-label case “clear”). However, compared with the impact of accounting for non-BC LAPs and snow depth, the impact of accounting for cloud cover on albedo reduction is much smaller. The differences in the albedo reduction induced by BC under clear sky and under cloudy sky are within 10–20% (Table 2).

As shown in Figure 12b, a low bias in BC concentration will lead to a proportional decrease in albedo reduction induced by BC; for example, if the BC concentration is reduced by a factor of 10, the albedo reduction induced by BC will be reduced by approximately a factor of 10 in China, North America, and the Arctic. In contrast, the albedo reduction induced by BC does not increase linearly with the increase of BC concentration. A factor of 10 increases in BC concentration leads to a factor of 4–7 increases in albedo reduction. Compared to North America and the Arctic, the relative increase in albedo reduction is smaller in China given the same relative increase in BC concentration, because snow in China already contains large amounts of BC.

Similarly, biases in snow depth will not yield proportional biases in albedo reduction. If the BC concentration is high or the snow grain size is small, a thin layer of snowpack could be optically thick (semi-infinite)—on average a photon cannot pass through the medium without being absorbed or reflected. In this case, although the increase of snow depth will increase the total optical depth of snowpack, it does not affect BC-in-snow albedo reduction since the snow was already optically thick enough. However, reducing snow depth may reduce the total optical depth enough that the snowpack is no longer semi-infinite—more photons could travel through the snowpack and escape without being absorbed or penetrate through the snowpack. Therefore, as illustrated in Figure 12b, for new snow, if the snow depth is decreased by a factor of 10, the albedo reduction induced by BC is decreased by only a factor of 4, 5, and 2 for the Arctic, North America, and China, respectively; if the snow depth is increased by a factor of 10, the albedo reduction induced by BC is increased by only a factor of 1.1 and 1.3 for the Arctic and North America, and almost no

Table 2. Relative Change ($\delta\Delta\alpha/\Delta\alpha$, Where $\delta\Delta\alpha = \Delta\alpha_{ST} - \Delta\alpha$, Blue Shading), and Absolute Change ($\delta\Delta\alpha, 10^{-4}$) in Albedo Reductions Induced by BC (All-Sky, Regional Mean) for Cases With Different Snow Depths (SD), Cloud Cover, and Concentrations of BC and Non-BC LAPs, for New Snow ($r = 100 \mu\text{m}$) and Old Snow ($r = 1000 \mu\text{m}$)

		Arctic				North America				China			
		$r = 100 \mu\text{m}$ (March)		$r = 1000 \mu\text{m}$ (April)		$r = 100 \mu\text{m}$ (February)		$r = 1000 \mu\text{m}$ (March)		$r = 100 \mu\text{m}$ (February)		$r = 1000 \mu\text{m}$ (March)	
Deep snow, BC only	Deep snow, BC only	28	0.91	123	2.54	37	1.47	168	5.68	280	1.05	920	2.23
	Deep snow	4	0.19	51	1.17	6	0.52	75	2.99	5	0.03	130	0.38
	BC only	13	0.32	10	0.11	14	0.29	9	0.07	208	0.7	301	0.51
	Clear sky	-4	-0.09	-8	-0.1	-4	-0.08	-7	-0.09	-16	-0.05	-37	-0.06
	Cloudy sky	3	0.08	6	0.07	3	0.07	5	0.06	22	0.07	44	0.08
Snow containing both BC and non-BC LAPs	BC \times 0.1	-40	-0.89	-77	-0.9	-42	-0.89	-77	-0.9	-274	-0.88	-505	-0.88
	0.2	-34	-0.78	-68	-0.79	-37	-0.78	-68	-0.79	-237	-0.76	-437	-0.77
	0.5	-20	-0.47	-41	-0.49	-22	-0.47	-42	-0.49	-138	-0.45	-253	-0.46
	2	35	0.82	74	0.92	38	0.82	77	0.92	221	0.75	389	0.75
	5	115	2.83	255	3.35	125	2.77	272	3.36	682	2.39	1123	2.33
	10	215	5.43	486	6.75	235	5.3	526	6.72	1185	4.28	1799	4.01
	SD \times 0.1	-31	-0.73	-73	-0.85	-37	-0.8	-77	-0.91	-160	-0.57	-457	-0.82
	0.2	-21	-0.53	-60	-0.71	-27	-0.63	-66	-0.8	-85	-0.33	-343	-0.65
	0.5	-7	-0.2	-30	-0.38	-11	-0.27	-37	-0.47	-20	-0.08	-140	-0.3
	2	3	0.11	27	0.44	4	0.15	38	0.59	5	0.02	89	0.23
5	4	0.17	45	0.89	6	0.28	66	1.23	5	0.03	127	0.37	
10	4	0.18	49	1.07	6	0.37	71	1.6	5	0.03	130	0.38	
Snow containing BC only	BC \times 0.1	-37	-0.83	-76	-0.88	-39	-0.84	-76	-0.89	-215	-0.7	-448	-0.79
	0.2	-30	-0.67	-65	-0.77	-32	-0.69	-66	-0.78	-143	-0.48	-334	-0.61
	0.5	-12	-0.26	-36	-0.43	-13	-0.28	-37	-0.45	16	0.05	-52	-0.13
	2	52	1.29	90	1.11	58	1.23	92	1.05	483	1.66	799	1.48
	5	138	3.51	280	3.7	154	3.37	299	3.61	1008	3.57	1663	3.36
	10	241	6.3	519	7.26	269	6.02	565	7.09	1549	5.63	2412	5.23
	SD \times 0.1	-30	-0.72	-73	-0.85	-36	-0.8	-77	-0.91	-139	-0.51	-445	-0.8
	0.2	-19	-0.5	-59	-0.71	-26	-0.61	-66	-0.8	-21	-0.16	-301	-0.58
	0.5	0	-0.05	-27	-0.35	-4	-0.15	-35	-0.45	129	0.37	13	-0.06
	2	21	0.6	51	0.72	27	0.62	65	0.84	252	0.9	571	1.14
5	26	0.81	93	1.54	34	0.9	125	1.9	273	1.01	800	1.78	
10	27	0.88	111	2.01	36	1.06	149	2.57	278	1.03	875	2.04	

increase in China. For old snow, the change in albedo reduction is more sensitive to the change of snow depth because the optical depth of old melting snow is smaller for the same snow thickness.

If the albedo calculation does not include non-BC LAPs, as illustrated in Figure 12c, the change in albedo reduction induced by BC is disproportional to the changes of BC concentration, because the removal of non-BC LAPs increases the BC-in-snow albedo reduction even if there is no increase of BC concentrations (Figure 12, case BC only). An increase of snow depth or BC concentration yields a much larger change in the albedo reduction, and the regional differences are smaller. It is important to note that even if we reduce the snow depth for China to 50% of the observed values, the derived albedo reduction by BC still increases by 40% for new snow and 6% for old snow relative to the case where the snowpack contains non-BC LAPs. This is because the concentrations of non-BC LAPs in snow are so high in China that the removal of non-BC LAPs greatly increases albedo reduction by BC, which compensates for the drop of albedo reduction due to shallower snowpacks.

3.4. Snow Depth Distribution

For the 22 sites in subarctic Canada, the mean and distributed snow depths are shown in Figure 13 (top). The mean snow depths are in the range 20 to 50 cm for all but three sites. If snow albedos were calculated using

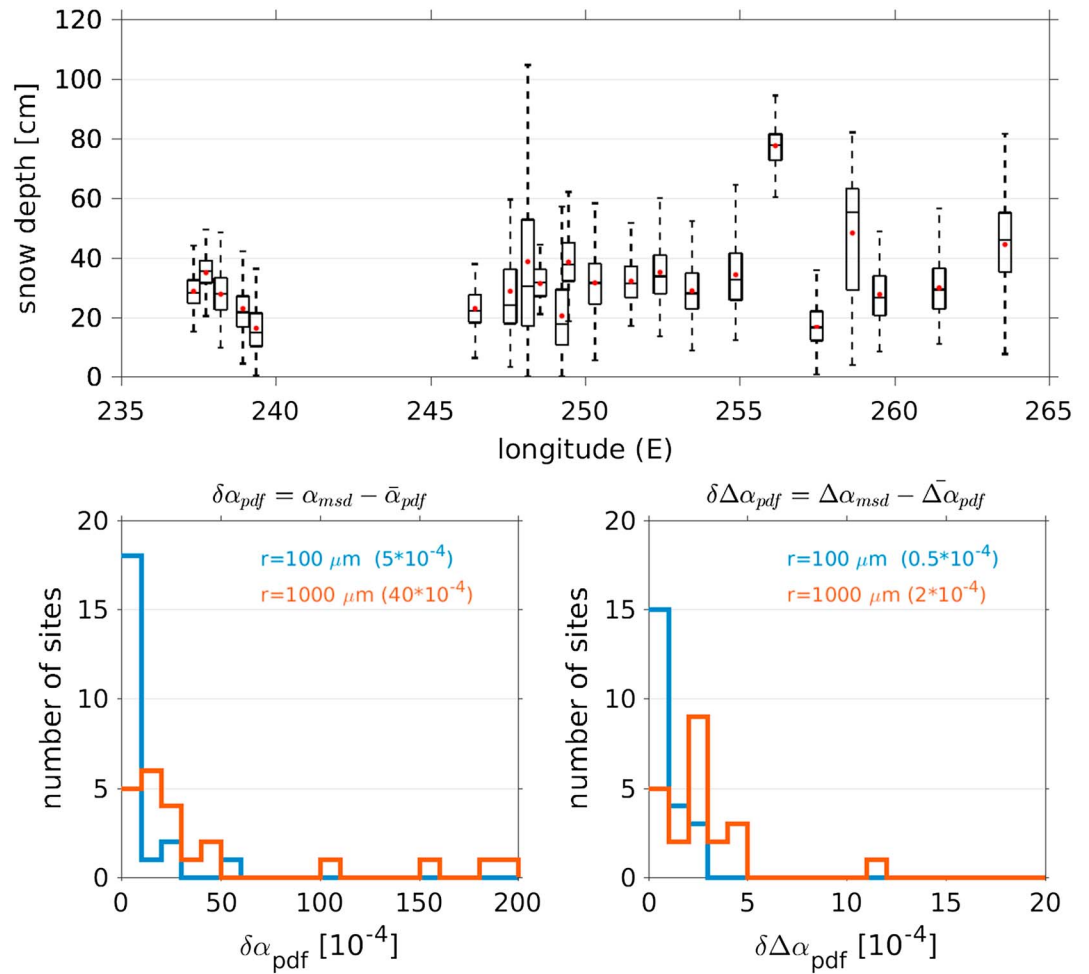


Figure 13. (top) Snow depth distribution measured at 22 sites in subarctic Canada (region outlined by black box in Figure 1). (bottom) Differences in snow albedo (α) and albedo reduction induced by BC ($\Delta\alpha$) between values derived from a snowpack with mean depth (α_{msd}) and mean values derived from snowpacks with distributed depths (α_{pdf}). Values in parentheses are site-averaged data.

site-mean snow depth, we could overestimate both snow albedo and albedo reduction by BC, as shown in the bottom panel of Figure 13. The mean albedos of snowpacks with distributed depths are smaller by 0.0005 and 0.0040 for new snow and old snow; the mean albedo reduction is also smaller by 5×10^{-5} and 0.0002 for new snow and old snow. However, these changes are much smaller than the albedo reduction by BC in the Arctic region: 0.0045 for new snow and 0.0087 for old snow. We conclude that for mean snow depths >20 cm, it is adequate for radiative computations to use the mean snow depths without consideration of the local depth-distribution.

4. Discussions and Summary

In this paper, we derived the direct albedo reduction induced by BC and non-BC LAPs in snow based on large-area field observations. We also investigated the impact of different snow conditions, LAP concentrations, and model setups on derived BC-in-snow albedo reductions. Comparisons of these quantities across three sampling regions are also highlighted.

Depending on the snow grain size, the direct albedo reductions caused by BC in the Arctic, North America, and China are 0.005, 0.005, and 0.031 for new snow and 0.01, 0.01, and 0.06 for old snow. These values can be used for future model simulations to constrain the direct albedo reduction induced by BC.

Correspondingly in the Arctic, North America, and China, the direct forcing by BC is 0.06, 0.3, and 3 W m^{-2} for new snow and 0.5, 0.8, and 7.5 W m^{-2} for old snow during the winter-spring transition. These forcings do not account for rapid adjustments (feedback). It is important to note that the direct radiative forcing induced by BC will be amplified through feedback processes that involve both the snow and atmosphere [Bond *et al.*, 2013, Figure 29]. These feedbacks are overwhelmingly positive, so the total effective radiative forcing induced by BC will be larger than the direct forcing estimated in this work.

To estimate the radiative forcing induced by BC in snow, it is important for model simulations to include non-BC LAPs as well. We find that non-BC LAPs are responsible for at least 50% of LAP-in-snow albedo reductions in our study regions (Table 1). The presence of non-BC LAPs in snow also reduces the amount of albedo reduction induced by BC. Simulations without non-BC LAPs in snow will therefore overestimate the albedo reduction by BC, especially in China (Figure 12 and Table 2). However, because some of the non-BC LAPs are emitted from anthropogenic sources, it is unclear whether the total direct forcing by anthropogenic LAPs in snow is overestimated.

Another factor that models should consider is snow depth. As shown in Figure 12, albedo reduction by BC increases by a factor of 1 to 3 if the snow is deeper than that measured a factor of 10; correspondingly, the impact of BC is smaller if snow depth is smaller than we measured at these sites. Regional-averaged BC-in-snow albedo reduction is less sensitive to the change of snow depth in China than in North America and the Arctic, since the BC concentration in China is higher (i.e., snowpacks are more likely to be optically thick). For regions with shallower snowpack and lower BC concentration, accurate representation of snow-covered fraction and snow depth distribution are especially important for calculations of regional forcing. In this work, we showed that the impact of snow-depth distribution on snow albedo and albedo reduction by BC at 22 sites in subarctic Canada was small. However, the snow is deep in this region. The impact of depth distribution might be larger in midlatitude regions where snow is shallower.

As stated in section 1, most studies testing modeled radiative forcing by BC in snow have focused on the simulated BC concentration in the surface snow layer. Those studies have shown that modeled BC concentrations can differ from observed concentrations by up to an order of magnitude. This error in BC concentration could yield a large error in derived albedo reduction by BC due to two reasons. First, the albedo reduction by BC is almost linear in BC concentration for the typical BC amounts we find (Figure 12). For example, doubling the amount of BC in snow would double the BC-in-snow albedo reduction for new snow in all three regions; such a change in BC-in-snow albedo reduction is larger if model simulations do not consider non-BC LAPs. Second, even if the modeled BC concentrations in the top layer agree with observations, the computed albedo reduction could be erroneous. At almost all sampling sites, the top layer (5 cm) is not optically thick enough to hide the impact of the lower snowpack or the ground below (Figure 11).

Based on this work, our suggestions for future field observations and model testing regarding BC-in-snow albedo reduction are summarized as follows:

1. In addition to measuring BC, field observations on LAPs in snow should also measure non-BC LAPs (i.e., BrC and MD). Ideally, both the mass and absorption properties of these constituents should be measured.
2. Measurements of snow depth distributions are needed, for both midlatitudes and the Arctic. Ideally, repeated snow depth distribution should be measured during both snow seasons and melting seasons to capture its temporal variation.
3. For long-term observations of LAPs in snow at fixed locations, if it is not feasible to repeatedly sample the entire snowpack in layers (e.g., according to the snow stratigraphy), at a minimum the surface snow (top 5 cm) and the bulk snow below should each be sampled.
4. It is important for radiative transfer models to include non-BC LAPs in snow.
5. Testing for accurate model simulations of snow depth (as well as snow depth distributions, if the snow is thin) is crucial to model estimates of forcing by BC/LAPs in snow.
6. If radiative transfer calculations assume a homogenous snowpack, mean concentrations of BC in the surface snow layer (5 cm) should be used as the proxy data to evaluate the model performance on BC-induced direct albedo reduction and forcing, rather than the mean concentrations of BC in the entire snow column.

By utilizing field observations, we were able to run our sensitivity studies using appropriate snow LAP concentrations and snow depths for the studied regions. Other sources of uncertainty in the snow albedo calculations were not observationally constrained. First, we had observed snow depth distributions and fractions for only one subregion—subarctic Canada. During our fieldwork snow sampling sites were selected to represent the snow conditions in the surrounding area, but we cannot quantify how representative the chosen site truly was. Second, we do not have repeated measurements at all sites to quantify the temporal variation of LAP concentration and snow conditions. The radiative forcing estimated in this work should be considered an estimate of the direct radiative forcing over snow at the beginning of melting season, before melt has commenced; it will not reflect that mean forcing through entire melting season. Further, we used mean cloud fractions (10 year climatology of 2005–2014) to estimate the all-sky radiative forcing; we have not quantified the uncertainty in forcing due to variations in cloud optical depth and cloud fraction. The last sources of uncertainties are associated with the radiative transfer calculation. If the size and density of ambient BC are different from our assumptions, the BC-induced albedo reduction might also be different. We also assume that LAPs and snow grains are mixed externally, while for natural snowpack, especially during melting season, LAPs are more likely to mixed internally with snow grains; in the latter case, the BC-in-snow forcing may increase substantially [Liou et al., 2014; He et al., 2014]. Snow grains in natural snowpacks are also not spherical, but we assumed spherical grains for the radiative transfer calculations. This could be a source of uncertainty if the effective snow grain radius were selected based on field measurements of grain size [Dang et al., 2016]; in our work, the effective snow grain radii for new snow (100 μm) and old snow (1000 μm) were picked based on matching radiative transfer calculations to measurements of snow albedo. Since they were then used in radiative transfer calculations, the snow grain size and shape is not a major source of uncertainty. It is important to note that the ambient snowpack grain sizes are determined by the atmospheric and snow conditions during and after snowfall and will vary within a snowpack. Here we opted to present results for the bounding cases of snow grain sizes typical of new snow and old snow throughout the whole snowpack. Lastly, we estimated the BC-in-snow radiative forcing without excluding BC emitted from non-anthropogenic sources. This assumption is not valid in nature [Hegg et al., 2009; Zhang et al., 2013, 2015]. The forcing values reported in this work should be considered as the maximum amount of BC-in-snow forcing given the observed snow conditions. Research works aiming at quantifying the radiative forcing of LAPs in snow should also include the impact of non-BC LAPs that are emitted from anthropogenic sources, which we do not address in this paper.

Acknowledgments

We thank Richard Brandt for providing the single-scattering properties of snow grains and black carbon particles from Mie calculations. We thank Hailong Wang and two anonymous reviewers for their insightful suggestions. This work was supported by National Science Foundation grant AGS-11-18460. The data are available at the following website: <http://hdl.handle.net/1773/39741>.

References

- Andreae, M. O., and A. Gelencsér (2006), Black carbon or brown carbon? The nature of light-absorbing carbonaceous aerosols, *Atmos. Chem. Phys.*, *6*, 3131–3148, doi:10.5194/acp-6-3131-2006.
- Aoki, T., H. Motoyoshi, Y. Kodama, T. J. Yasunari, K. Sugiura, and H. Kobayashi (2006), Atmospheric aerosol deposition on snow surfaces and its effect on albedo, *SOLA*, *2*, 13–16.
- Aoki, T., K. Kuchiki, M. Niwano, Y. Kodama, M. Hosaka, and T. Tanaka (2011), Physically based snow albedo model for calculating broadband albedos and the solar heating profile in snowpack for general circulation models, *J. Geophys. Res.*, *116*, D11114, doi:10.1029/2010JD015507.
- Bøggild, C. E., R. E. Brandt, K. J. Brown, and S. G. Warren (2010), The ablation zone in northeast Greenland: Ice types, albedos, and impurities, *J. Glaciol.*, *56*, 101–113.
- Bond, T. C., and R. W. Bergstrom (2006), Light absorption by carbonaceous particles: An investigative review, *Aerosol Sci. Technol.*, *40*(1), 27–67.
- Bond, T. C., D. G. Streets, K. F. Yarber, S. M. Nelson, J.-H. Woo, and Z. Klimont (2004), A technology-based global inventory of black and organic carbon emissions from combustion, *J. Geophys. Res.*, *109*, D14203, doi:10.1029/2003JD003697.
- Bond, T. C., et al. (2013), Bounding the role of black carbon in the climate system: A scientific assessment, *J. Geophys. Res. Atmos.*, *118*, 1–173, doi:10.1002/jgrd.50171.
- Brandt, R. E., S. G. Warren, A. P. Worby, and T. C. Grenfell (2005), Surface albedo of the Antarctic sea ice zone, *J. Clim.*, *18*(17), 3606–3622.
- Charlson, R. J., S. E. Schwartz, J. M. Hales, R. D. Cess, J. A. Coakley Jr., J. E. Hansen, and D. J. Hoffman (1992), Climate forcing by anthropogenic aerosols, *Science*, *255*, 423–430, doi:10.1126/science.255.5043.423.
- Clarke, A. D., and K. J. Noone (1985), Soot in the Arctic snowpack: A cause for perturbations in radiative transfer, *Atmos. Environ.*, *19*, 2045–2053.
- Clarke, A. D., K. J. Noone, J. Heintzenberg, S. G. Warren, and D. S. Covert (1987), Aerosol light absorption measurement techniques: Analysis and intercomparisons, *Atmos. Environ.*, *21*, 1455–1465.
- Dang, C., and D. A. Hegg (2014), Quantifying light absorption by organic carbon in Western North American snow by serial chemical extractions, *J. Geophys. Res. Atmos.*, *119*, 10,247–10,261, doi:10.1002/2014JD022156.
- Dang, C., R. E. Brandt, and S. G. Warren (2015), Parameterizations for narrowband and broadband albedo of pure snow and snow containing mineral dust and black carbon, *J. Geophys. Res. Atmos.*, *120*, 5446–5468, doi:10.1002/2014JD022646.
- Dang, C., Q. Fu, and S. G. Warren (2016), Effect of snow grain shape on snow albedo, *J. Atmos. Sci.*, *73*, 3573–3583, doi:10.1175/JAS-D-15-0276.1.

- Doherty, S. J., S. G. Warren, T. C. Grenfell, A. D. Clarke, and R. E. Brandt (2010), Light-absorbing impurities in Arctic snow, *Atmos. Chem. Phys.*, *10*(23), 11,647–11,680.
- Doherty, S. J., T. C. Grenfell, S. Forsström, D. L. Hegg, R. E. Brandt, and S. G. Warren (2013), Observed vertical redistribution of black carbon and other insoluble light-absorbing particles in melting snow, *J. Geophys. Res. Atmos.*, *118*, 5553–5569, doi:10.1002/jgrd.50235.
- Doherty, S. J., C. Dang, D. A. Hegg, R. Zhang, and S. G. Warren (2014), Black carbon and other light-absorbing particles in snow of central North America, *J. Geophys. Res. Atmos.*, *119*, 12,807–12,831, doi:10.1002/2014JD022350.
- Doherty, S. J., D. A. Hegg, J. E. Johnson, P. K. Quinn, J. P. Schwarz, C. Dang, and S. G. Warren (2016), Causes of variability in light absorption by particles in snow at sites in Idaho and Utah, *J. Geophys. Res. Atmos.*, *121*, 4751–4768, doi:10.1002/2015JD024375.
- Flanner, M. G., C. S. Zender, J. T. Randerson, and P. J. Rasch (2007), Present-day climate forcing and response from black carbon in snow, *J. Geophys. Res.*, *112*, D11202, doi:10.1029/2006JD008003.
- Flanner, M. G., C. S. Zender, P. G. Hess, N. M. Mahowald, T. H. Painter, V. Ramanathan, and P. J. Rasch (2009), Springtime warming and reduced snow cover from carbonaceous particles, *Atmos. Chem. Phys.*, *9*, 2481–2497.
- Grenfell, T. C., and D. K. Perovich (2008), Incident spectral irradiance in the Arctic Basin during the summer and fall, *J. Geophys. Res.*, *113*, D12117, doi:10.1029/2007JD009418.
- Grenfell, T. C., S. G. Warren, and P. C. Mullen (1994), Reflection of solar radiation by the Antarctic snow surface at ultraviolet, visible, and near-infrared wavelengths, *J. Geophys. Res.*, *99*, 18,669–18,684, doi:10.1029/94JD01484.
- Grenfell, T. C., S. J. Doherty, A. D. Clarke, and S. G. Warren (2011), Light absorption from particulate impurities in snow and ice determined by spectrophotometric analysis of filters, *Appl. Opt.*, *50*, 2037–2048.
- Hansen, J., and L. Nazarenko (2004), Soot climate forcing via snow and ice albedos, *Proc. Natl. Acad. Sci. U.S.A.*, *101*, 423–428.
- He, C., Q. Li, K. N. Liou, Y. Takano, Y. Gu, L. Qi, Y. Mao, and L. R. Leung (2014), Black carbon radiative forcing over the Tibetan Plateau, *Geophys. Res. Lett.*, *41*, 7806–7813, doi:10.1002/2014GL062191.
- Hegg, D. A., S. G. Warren, T. C. Grenfell, S. J. Doherty, T. V. Larson, and A. D. Clarke (2009), Source attribution of black carbon in Arctic snow, *Environ. Sci. Technol.*, *43*(11), 4016–4021.
- Huang, J., Q. Fu, W. Zhang, X. Wang, R. Zhang, H. Ye, and S. G. Warren (2011), Dust and black carbon in seasonal snow across northern China, *Bull. Am. Meteorol. Soc.*, *92*(2), 175–181.
- Jacobson, M. Z. (2004), Climate response of fossil fuel and biofuel soot, accounting for soot's feedback to snow and sea ice albedo and emissivity, *J. Geophys. Res.*, *109*, D21201, doi:10.1029/2004JD004945.
- Kirchstetter, T. W., T. Novakov, and P. V. Hobbs (2004), Evidence that the spectral dependence of light absorption by aerosols is affected by organic carbon, *J. Geophys. Res.*, *109*, D21208, doi:10.1029/2004JD004999.
- Koch, D., and A. D. Del Genio (2010), Black carbon absorption effects on cloud cover: Review and synthesis, *Atmos. Chem. Phys.*, *10*, 7685–7696, doi:10.5194/acp-10-7685-2010.
- Koch, D., S. Menon, A. DelGenio, R. Ruedy, I. Alienov, and G. A. Schmidt (2009), Distinguishing aerosol impacts on climate over the past century, *J. Clim.*, *22*, 2659–2677, doi:10.1175/2008JCLI2573.1.
- Liang, S., H. Fang, M. Chen, C. Walthall, C. Daughtry, J. Morisette, C. Schaaf, and A. Strahler (2002), Validating MODIS land surface reflectance and albedo products: Methods and preliminary results, *Remote Sens. Environ.*, *83*(1–2), 149–162.
- Liou, K. N., Y. Takano, C. He, P. Yang, R. L. Leung, Y. Gu, and W. L. Lee (2014), Stochastic parameterization for light absorption by internally mixed BC/dust in snow grains for application to climate models, *J. Geophys. Res. Atmos.*, *119*, 7616–7632, doi:10.1002/2014JD021665.
- Marshall, S. E. (1989), *A Physical Parameterization of Snow Albedo for Use in Climate Models*, NCAR Cooperative Thesis, vol. 123, 175 pp., Natl. Cent. for Atmos. Res., Boulder, Colo.
- Moosmüller, H., R. K. Chakrabarty, and W. P. Arnott (2009), Aerosol light absorption and its measurement: A review, *J. Quant. Spectrosc. Radiat. Transfer*, *110*(11), 844–878.
- Namazi, M., K. von Salzen, and J. N. S. Cole (2015), Simulation of black carbon in snow and its climate impact in the Canadian Global Climate Model, *Atmos. Chem. Phys.*, *15*, 10,887–10,904, doi:10.5194/acp-15-10887-2015.
- Painter, T. H., A. P. Barrett, C. C. Landry, J. C. Neff, M. P. Cassidy, C. R. Lawrence, K. E. McBride, and G. L. Farmer (2007), Impact of disturbed desert soils on duration of mountain snow cover, *Geophys. Res. Lett.*, *34*, L12502, doi:10.1029/2007GL030284.
- Qian, Y., W. I. Gustafson Jr., L. Y. R. Leung, and S. J. Ghan (2009), Effects of soot-induced snow albedo change on snowpack and hydrological cycle in western United States based on Weather Research and Forecasting chemistry and regional climate simulations, *J. Geophys. Res.*, *114*, D03108, doi:10.1029/2008JD011039.
- Qian, Y., M. G. Flanner, L. Y. R. Leung, and W. Wang (2011), Sensitivity studies on the impacts of Tibetan Plateau snowpack pollution on the Asian hydrological cycle and monsoon climate, *Atmos. Chem. Phys.*, *11*(5), 1929–1948, doi:10.5194/acp-11-1929-2011.
- Qian, Y., H. Wang, R. Zhang, M. G. Flanner, and P. J. Rasch (2014), A sensitivity study on modeling black carbon in snow and its radiative forcing over the Arctic and Northern China, *Environ. Res. Lett.*, *9*(6), 064001, doi:10.1088/1748-9326/9/6/064001.
- Qian, Y., T. J. Yasunari, S. J. Doherty, M. G. Flanner, W. K. Lau, J. Ming, H. Wang, M. Wang, S. G. Warren, and R. Zhang (2015), Light-absorbing particles in snow and ice: Measurement and modeling of climatic and hydrological impact, *Adv. Atmos. Sci.*, *32*(1), 64–91.
- Ricchiazzi, P., S. Yang, C. Gautier, and D. Sowle (1998), SBDART: A research and teaching software tool for plane-parallel radiative transfer in the Earth's atmosphere, *Bull. Am. Meteorol. Soc.*, *79*(10), 2101–2114.
- Stamnes, K., S.-C. Tsay, W. Wiscombe, and K. Jayaweera (1988), Numerically stable algorithm for discrete-ordinate-method radiative transfer in multiple scattering and emitting layered media, *Appl. Opt.*, *27*(12), 2502–2509.
- Sturm, M., C. Derksen, G. Liston, A. Silis, D. Solie, J. Holmgren, and H. Huntington (2008), *A Reconnaissance Snow Survey Across Northwest Territories and Nunavut, Canada, April 2007* (ERDC/CRREL-TR-08-3), Cold Regions Research and Engineering Laboratory (CRREL), Hanover, N. H.
- Wang, M., et al. (2015), Carbonaceous aerosols recorded in a southeastern Tibetan glacier: Analysis of temporal variations and model estimates of sources and radiative forcing, *Atmos. Chem. Phys.*, *15*(3), 1191–1204.
- Wang, X., S. J. Doherty, and J. Huang (2013), Black carbon and other light-absorbing impurities in snow across Northern China, *J. Geophys. Res. Atmos.*, *118*, 1471–1492, doi:10.1029/2012JD018291.
- Warren, S. G., and R. E. Brandt (2008), Optical constants of ice from the ultraviolet to the microwave: A revised compilation, *J. Geophys. Res.*, *113*, D14220, doi:10.1029/2007JD009744.
- Warren, S. G., and W. J. Wiscombe (1980), A model for the spectral albedo of snow. II: Snow containing atmospheric aerosols, *J. Atmos. Sci.*, *37*, 2734–2745.
- Warren, S. G., and W. J. Wiscombe (1985), Dirty snow after nuclear war, *Nature*, *313*, 467–470.
- Wielicki, B. A., B. R. Barkstrom, E. F. Harrison, R. B. Lee III, G. L. Smith, and J. E. Cooper (1996), Clouds and the Earth's Radiant Energy System (CERES): An Earth observing system experiment, *Bull. Am. Meteorol. Soc.*, *77*(5), 853–868.

- Wiscombe, W. J., and S. G. Warren (1980), A model for the spectral albedo of snow. I: Pure snow, *J. Atmos. Sci.*, *37*, 2712–2733.
- Ye, H., R. Zhang, J. Shi, J. Huang, S. G. Warren, and Q. Fu (2012), Black carbon in seasonal snow across northern Xinjiang in northwestern China, *Environ. Res. Lett.*, *7*(4) 044002.
- Zhang, R., D. A. Hegg, J. Huang, and Q. Fu (2013), Source attribution of insoluble light-absorbing particles in seasonal snow across northern China, *Atmos. Chem. Phys.*, *13*(12), 6091–6099.
- Zhang, R., H. Wang, D. A. Hegg, Y. Qian, S. J. Doherty, C. Dang, P. L. Ma, P. J. Rasch, and Q. Fu (2015), Quantifying sources of black carbon in western North America using observationally based analysis and an emission tagging technique in the Community Atmosphere Model, *Atmos. Chem. Phys.*, *15*, 12,805–12,822, doi:10.5194/acp-15-12805-2015.
- Zhao, C., et al. (2014), Simulating black carbon and dust and their radiative forcing in seasonal snow: A case study over North China with field campaign measurements, *Atmos. Chem. Phys.*, *14*, 11,475–11,491, doi:10.5194/acp-14-11475-2014.